The Astrophysical Journal Letters, 776:L8 (4pp), 2013 October 10 doi:10.1088/2041-8205/776/1/L8

ASSOCIATION OF SUPRATHERMAL PARTICLES WITH COHERENT STRUCTURES AND SHOCKS

J. A. Tessein[1], W. H. Matthaeus[1], M. Wan[1], K. T. Osman[2], D. Ruffolo[3,4], and J. Giacalone[5]
[1] Department of Physics and Astronomy, University of Delaware, Newark, DE 19716, USA
[2] Centre for Fusion, Space and Astrophysics, University of Warwick, Coventry CV4 7AL, UK
[3] Department of Physics, Faculty of Science, Mahidol University, Bangkok 10400, Thailand
[4] Thailand Center of Excellence in Physics, CHE, Ministry of Education, Bangkok 10400, Thailand
[5] Department of Planetary Sciences and Lunar and Planetary Laboratory, University of Arizona, 1629 East University Boulevard, Tucson, AZ 85721, USA
Received 2013 July 3; accepted 2013 August 26; published 2013 September 25

ABSTRACT

Various mechanisms have been proposed to explain observed suprathermal particle populations in the solar wind, including direct acceleration at flares, stochastic acceleration, shock acceleration, and acceleration by random compression or reconnection sites. Using magnetic field and suprathermal particle data from the *Advanced Composition Explorer* (*ACE*), we identify coherent structures and interplanetary shocks, and analyze the temporal association of energetic particle fluxes with these coherent structures. Coherent structures having a range of intensities are identified using the magnetic Partial Variance of Increments statistic, essentially a normalized vector increment. A stronger association of energetic particle flux in the 0.047–4.75 MeV range is found with intense magnetic discontinuities than is found with shocks. Nevertheless, the average profile of suprathermals near shocks is quite consistent with standard models of diffusive shock acceleration, while a significant amount of the energetic particles measured and strong discontinuities are found by *ACE* within six hours of a shock. This evidence supports the view that multiple mechanisms contribute to the acceleration and transport of interplanetary suprathermal particles.

Key words: acceleration of particles – magnetohydrodynamics (MHD) – plasmas – shock waves – solar wind

1. INTRODUCTION

Suprathermal particles are an important ingredient of the solar system environment, representing a fundamental feature of dynamically active low collisionality astrophysical plasmas, and providing keys to understanding energetically important solar system phenomena such as flares, coronal mass ejections (CMEs), and associated production of energetic particles (Reames 1999; Zweibel & Yamada 2009; Park et al. 2012), while also representing an influential component of space weather variations that impact technological and societal assets on the ground and in space (Lanzerotti 2001). Various mechanisms have been proposed for the acceleration of the solar wind suprathermal particle populations, including shock acceleration, stochastic acceleration, and acceleration due to random reconnection sites and compressions (Melrose 1968; Matthaeus et al. 1984; Drake et al. 2006; Fisk & Gloeckler 2006; Drake et al. 2009). Some particles are solar energetic particles (SEPs) which are strongly associated with disturbances originating at the Sun, and these are typically associated either with diffusive shock acceleration, for so-called gradual SEP events (Giacalone 2012), or direct acceleration at large reconnection sites, which has been the process most frequently associated with impulsive SEP events. There also is evidence (Gloeckler et al. 2000) for a more distributed production of heliospheric suprathermal particles, possibly associated with random reconnection events or random compressions (Fisk & Gloeckler 2006). Unraveling the sources responsible for particular observed "events" is made more complex by the possibility, or indeed likelihood, that both diffusive transport effects, as well as nondiffusive transport effects, akin to observed dropouts (Mazur et al. 2000) can provide conduits for coherent communication of nonthermal particles over large distances in the interplanetary medium. Rather than seeking evidence in support of a single interpretation, here we report an analysis of suprathermal particle observations based on conditional statistics and local averaging to provide a baseline understanding of the relative importance of contribution of coherent structures, shocks, and homogeneous processes in observed suprathermal enhancements. A perhaps unanticipated result is that the average intensities of suprathermal particles at or near strong coherent structures, e.g., discontinuities, is greater than the average value near interplanetary shocks.

Among the several approaches to particle acceleration, there is a great variation in the anticipated role of coherent magnetic structures. These include shocks, directional discontinuities, and active reconnection sites (Servidio et al. 2011), and are an integral ingredient of intermittent turbulence (Bruno et al. 2001; Hada et al. 2003). The Partial Variance of Increments (PVI) method (see below) is a useful way to identify these "events" in a numerical or observational dataset (Greco et al. 2009). The classical flare scenario involves acceleration at an intense reconnection event typically viewed as highly localized. Ingredients in diffusive shock acceleration are the shock itself, which is one type of coherent entity, as well as the nearby turbulence required to scatter the particles repeatedly across the shock. This turbulence is likely to be intermittent, i.e., admit a statistical hierarchy of coherent structures. Acceleration by random encounters with small reconnection sites appears to require structure, while it is less obvious that encounters with random compressions (Fisk & Gloeckler 2006; Jokipii & Lee 2010; Schwadron et al. 2010) requires coherent structure to be present. On the other hand, standard stochastic acceleration in which particles scatter between packets of random phased waves seems to avoid the issue of coherent structures entirely.

While it is completely plausible from a theoretical perspective that coherent structures may be involved in underlying acceleration mechanisms, the connection between the associated structures and observed statistical features of intermittency in turbulence has not typically been viewed as a central observational issue. One interesting exception is the channeling or

Table 1
Summary of the Data Used

Instrument	Measurement	Energy Range	Cadence	Time Interval
ACE/EPAM/LEMS30	Ion flux	0.047–4.75 MeV	5 minutes	1998-23 to 2010-258
ACE/SWEPAM	Plasma parameters	0.26–36 keV	64 s	1998-23 to 2010-258
ACE/MAG	Magnetic field	N/A	64 s	1998-23 to 2010-258

dropout of energetic particle fluxes seen in SEP data (Giacalone et al. 2000; Ruffolo et al. 2003; Chollet & Giacalone 2008, 2011; Trenchi et al. 2013). These sudden drops of particle counts may delineate boundaries, either flux tube boundaries, or perhaps more precisely, trapping boundaries, which are related to magnetic structure and phase coherence (Giacalone et al. 2000; Ruffolo et al. 2003; Zimbardo et al. 2004; Seripienlert et al. 2010). Meanwhile, recent investigations of heating and dissipation in the solar wind plasma have emphasized the potential importance of coherent magnetic structures. Studies have found increased heating and evidence of plasma instabilities at and near coherent structures such as current sheets (Osman et al. 2011, 2012a, 2012b; Wu et al. 2013). Here we will employ similar methods based on conditional statistics to ask whether there is an association of structures with suprathermal particle fluxes.

2. DATA AND ANALYSIS PROCEDURES

The data employed are from the *Advanced Composition Explorer* (*ACE*) spacecraft and are summarized in Table 1. We use data from the EPAM/LEMS30 sensor for suprathermal ions in the energy range 0.047–4.75 MeV (Gold et al. 1998). The *ACE* merged MAG/SWEPAM 64 s dataset was used for magnetic field data, to calculate the PVI statistics (see below), and for plasma density data (McComas et al. 1998; Smith et al. 1998). In the analyses that involve shocks, we employ the *ACE* shocks listing (posted at the ACE Science Center). This database gives additional information about the shocks observed by *ACE*, e.g., Mach number and shock angle. SWEPAM data provides three-component magnetic field, three-component proton velocity, proton temperature, proton density, magnetic field angle, and alpha-to-proton-number density ratio. The EPAM instrument provides flux of energetic particles. The 5 minute *ACE*/EPAM (energetic particles) and merged 64 s *ACE* MAG/SWEPAM (plasma parameters) have been merged (not decimated) to 5 minutes time resolution. We analyze the total flux of the LEMS30 instrument summed over all eight energy channels for the quantitative measure of energetic particle intensity that is used here. The analysis was repeated with data from the LEMS120 sensor, which gave very similar results (not shown here).

The PVI method is a simple and convenient way to locate coherent structures. It identifies discontinuities and other structures by scanning a time series for increments large enough that they are likely related to non-Gaussian events and intermittency (Greco et al. 2009). In particular, the method computes the quantity

$$\mathfrak{F} = \frac{|\Delta \mathbf{B}|}{\sqrt{\Sigma^2}} \quad (1)$$

where $\Sigma^2 = \langle |\Delta \mathbf{B}|^2 \rangle$ and $\Delta \mathbf{B}$ is increment $\mathbf{B}(t+\tau) - \mathbf{B}(t)$, and selects for values of $\mathfrak{F}$ greater than a specified threshold. The value of τ used for all results shown is five minutes, which corresponds to a scale within the inertial range of solar wind turbulence at 1 AU. The mean square value Σ^2 is computed over a large data sample. Data values with $\mathfrak{F} > 3$ or greater lie in the "tail" regions of the non-Gaussian distributions of increments that characterize intermittency. Increasing the threshold selects rare events with sharper gradients. Similar results can probably be obtained with other identification methods, such as Local Intermittency Measure, phase coherence method, or wavelets, which adopt related strategies. (Bruno et al. 2001; Hada et al. 2003) We prefer PVI due to its simplicity, ready implementation for either simulations or spacecraft data (Greco et al. 2009) and straightforward relation to intermittency statistics.

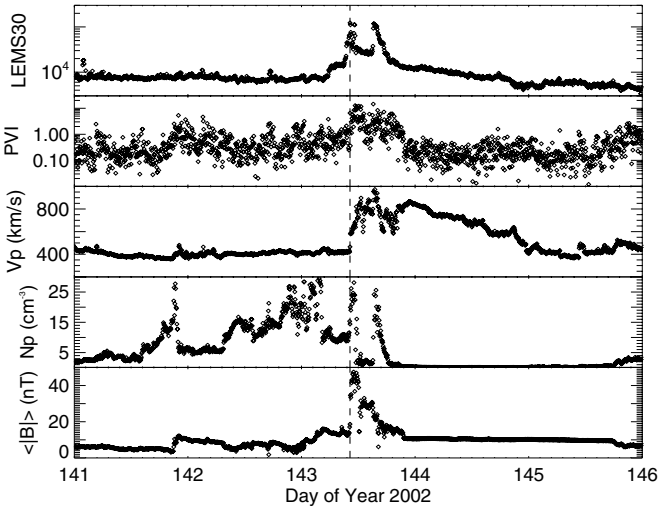

Figure 1. Sample event around a strong shock ($M_A > 4$, denoted by the vertical dashed line) with time series of energetic particle flux, PVI, density and magnetic field strength in the shock vicinity. There is a local peak of activity in PVI and energetic particles at the position of the shock; however, there are concurrent, higher values of intensities in both quantities at several downstream points.

3. RESULTS

Before examining statistics, we discuss some features of a particular interval, as illustrated in Figure 1. Given that there is so much variability in the SEP data, shock data, and magnetic field data, we are reluctant to state that this interval is typical, but a reasonable statement is that this interval displays several features that are frequently seen near shocks. This summary plot shows *ACE* data within about two days of a strong ($M_A > 4$) shock. The time series are energetic particle flux, PVI, density and magnetic field strength in the shock vicinity.

Figure 2 is the average energetic particle flux per PVI bin plotted against PVI threshold with and without shocks. For the case without shocks, the data six hours before and after the shock have been removed. The shock-associated intervals account for 7% of the total data. On these plots the errors of the mean are smaller than the plot symbols due to the large amount of data in the sample. For both cases, the averages of energetic particle flux and PVI threshold are strongly correlated, indicating a higher probability of finding a high energetic particle flux at an intense coherent structure. It is also apparent, noting the smaller magnitudes of the averaged particle fluxes with shocks

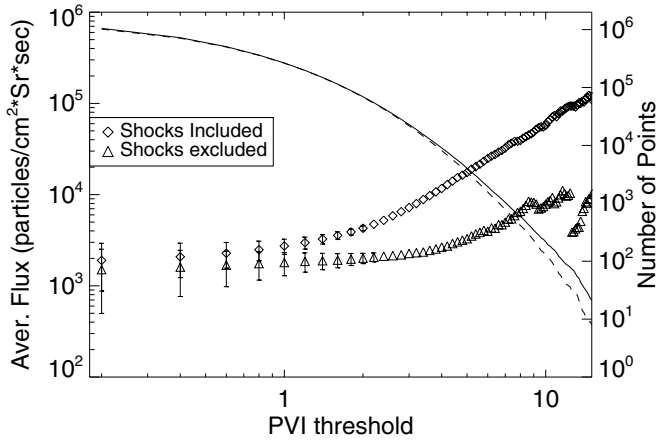

Figure 2. EPAM/LEMS30 average energetic particle flux plotted against PVI threshold with and without shocks. In the case without shocks, we removed from the analysis all the data six hours before and after the shocks. There are 100 PVI bins and the errors of the mean are mostly smaller than the plot symbols. The number of samples (right axis) for each PVI threshold is shown for all data (solid line) and for data excluding shocks (dashed line).

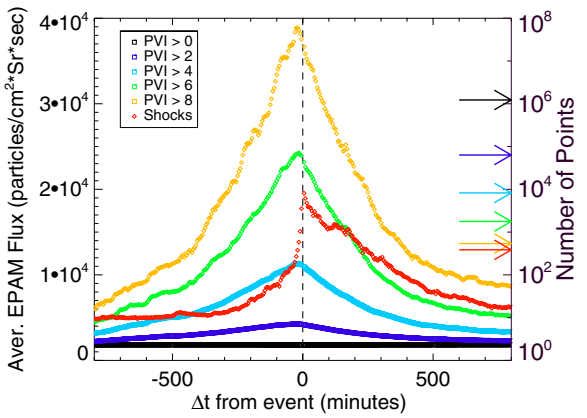

Figure 3. Average energetic particle flux conditioned on PVI and temporal proximity to the shock or PVI event for the cases with shocks included (analogous to Figure 1 from Osman et al. 2012b). There are 400 time bins and the errors of the mean are smaller than the plot symbols.

removed, that a significant amount of the energetic particles measured by *ACE* are within six hours of a shock.

Figures 3 and 4 depict the average energetic particle flux conditioned on PVI and temporal proximity to the shock or PVI event, for the case with all data included, and for the case in which data within six hours of the shocks have been removed. Note that this analysis is analogous to Figure 1 of Osman et al. (2012b) where heating in the proximity of discontinuities (PVI events) was examined. The expected errors of the mean in these figures are smaller than the plot symbols. There is a clear trend showing decreasing energetic particle flux as one moves farther from the magnetic discontinuity or shock. There is a peak in energetic particles at the PVI event and at the shock events—one should bear in mind that shocks are also a type of discontinuity. The peak average energetic particle flux for the shock events is comparable to the results for all PVI events in the range $4 < \mathfrak{F} < 6$. This may be because of the tendency of PVI events to cluster together. Thus, if strong PVI events are associated with higher energetic particle flux, one might expect higher energetic particle flux near the PVI event because of this clustering. Alternatively, it is possible that certain mechanisms for accelerating particles preferentially operate near (but not in) coherent structures (Dmitruk et al.

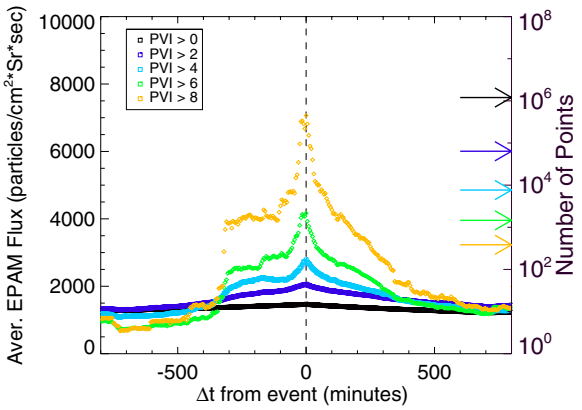

Figure 4. Average energetic particle flux conditioned on PVI and temporal proximity to the PVI event for the case with data removed within ±6 hr of shocks. There are 400 time bins and the errors of the mean are smaller than the plot symbols.

2004). The shape of the energetic particle distribution observed near the shock events is quite typical of what is expected from diffusive shock acceleration models. For the idealized case, one anticipates an exponential increase moving toward the shock from the upstream side of the shock. Downstream, one ideally expects a plateau region (Giacalone 2012), but this can be modified by escape mechanisms and non-planar shock effects.

Beyond the consistency of the shock profile with the diffusive shock acceleration model, the outstanding feature of the results in Figure 3 is that the average profiles with higher PVI (>6 and >8) have peaks that are well above the profile conditioned on shock events. In fact, the $\mathfrak{F} > 8$ profile peaks at a value more than 100% higher than the set of shocks. In the case with data near shocks removed, the $\mathfrak{F} > 8$ energetic particle peak is strong, but reaches values only about one-third of the shock peak average value.

All of the results shown above have been repeated using hydrogen and helium from *ACE*/SEPICA with similar results during the period of 1998 day 50 through 2001 day 357. The analysis shown here has also been performed with electrons with similar results.

4. CONCLUSIONS

The observed average profile of 322 shocks supports the prevailing view that diffusive shock acceleration contributes significantly to observed interplanetary suprathermal particles. However, the presence of still stronger energetic particle signals when the conditioning is done for stronger coherent structures ($\mathfrak{F} > 6$) is intriguing and points to the possible presence of other powerful acceleration mechanisms. Interestingly, the PVI-conditioned analysis on the data with shock neighborhoods removed also shows strong peaks, but at values less than both the shocks and the PVI cases with all data included. This confirms the fact that many of the stronger discontinuities occur in the few hours after a shock. The reasons that this should be so are very clear—shocks occur when faster wind overtakes slower wind, whether due to co-rotation CMEs or other large scale events. However, these are also ideal conditions for generating stronger magnetic field and turbulence, from compression (and associated amplification) as well as from nonlinear instability, e.g., due to shear. This is analogous to the reason that Alfvénic fluctuations disappear more rapidly in the inner heliosphere in stream interaction regions (see, e.g., Roberts et al. 1991). Therefore, one reasonably expects that enhanced intermittent

turbulence and cascade in the hours following a shock would also contain more coherent structures.

This leaves open the question as to why strong PVI events are seen to have a statistical association with enhanced suprathermal particles. This question is not readily answered as it requires that several known possibilities be addressed. There are two main categories of potential explanations. First, the particles seen at PVI events might be energized locally, due to reconnection events, current sheet activity, compressional acceleration, or related mechanisms (Ambrosiano et al. 1988; Le Roux et al. 2001; Dmitruk et al. 2004; Fisk & Gloeckler 2006; Schwadron et al. 2010). Indeed, we cannot at this time rule out that the observed enhancements are related to the commonly observed power-law spectrum of suprathermal heliospheric particles (Gloeckler 2003). The second possibility is that suprathermal enhancements near current sheets or similar coherent magnetic structures might be due to transport effects. Effects of magnetic connectivity have been investigated in the context of SEP dropouts (Ruffolo et al. 2003; Seripienlert et al. 2010), and chromospheric moss (Kittinaradorn et al. 2009). Another possibility is that compressions in the solar wind (e.g., when N_p peaks downstream of the shock in Figure 1) may form rapidly enough to compress the suprathermal particle distribution faster than it equilibrates due to particle diffusion, causing a coincidence between peaks in PVI and particle flux. In this way, the association of enhanced particle fluxes with magnetic structures could signify transport effects, while the acceleration itself occurs at a some remote location, perhaps lower in the corona, or at a more distant shock location. More detailed examination of available energetic particle data will be required to untangle these and perhaps other possibilities, motivated by the present demonstration that an interesting connection exists between suprathermal particles and coherent structures in the interplanetary magnetic field.

This research supported in part by the NSF SHINE (AGS-1156094) and Solar Terrestrial (AGS-1063439) Programs, and by NASA through the Magnetosphere Multiscale Mission Theory and Modeling program NNX08AT76G, and the Solar Probe Plus ISIS project, and by the "Turboplasmas" project (Marie Curie FP7 PIRSES-2010-269297) at the University of Calabria, and by the Thailand Research Fund, and UK STFC. The data has been obtained from the National Space Science Data Center http://nssdcftp.gsfc.nasa.gov and the ACE Science Center. The shocks used are from the *ACE* shocks listing. The authors acknowledge useful conversation with P. Blasi.

REFERENCES

Ambrosiano, J. J., Lee, L. C., & Swift, D. W. 1988, JGRA, 93, 14383
Bruno, R., Carbone, V., Veltri, P., Pietropaolo, E., & Bavassano, B. 2001, P&SS, 49, 1201
Chollet, E., & Giacalone, J. 2008, ApJ, 688, 1368
Chollet, E., & Giacalone, J. 2011, ApJ, 728, 64
Dmitruk, P., Matthaeus, W. H., & Seenu, N. 2004, ApJ, 617, 667
Drake, J., Swisdak, M., Phan, T., et al. 2009, JGR, 114, A05111
Drake, J. F., Swisdak, M., Che, H., & Shay, M. A. 2006, Natur, 443, 553
Fisk, L. A., & Gloeckler, G. 2006, ApJL, 640, L79
Giacalone, J. 2012, ApJ, 761, 28
Giacalone, J., Jokipii, J. R., & Mazur, J. 2000, ApJL, 532, L75
Gloeckler, G. 2003, in AIP Conf. Proc. 679, Solar Wind Ten, ed. M. Velli, R. Bruno, & F. Malara (Melville, NY: AIP), 583
Gloeckler, G., Fisk, L. A., Zurbuchen, T. H., & Schwadron, N. A. 2000, in Acceleration and Transport of Energetic Particles Observed in the Heliosphere, Vol. 528, ed. R. A. Mewaldt, J. R. Jokipii, M. A. Lee, E. Möbius, & T. H. Zurbuchen (Melville, NY: AIP), 221
Gold, R. E., Krimigis, S. M., Hawkins, S. E., III, et al. 1998, SpSciRev, 86, 541
Greco, A., Matthaeus, W. H., Servidio, S., Chuychai, P., & Dmitruk, P. 2009, ApJL, 691, L111
Hada, T., Koga, D., & Yamamoto, E. 2003, SSRv, 107, 463
Jokipii, J. R., & Lee, M. A. 2010, ApJ, 713, 475
Kittinaradorn, R., Ruffolo, D., & Matthaeus, W. H. 2009, ApJL, 702, L138
Lanzerotti, L. J. 2001, in Space Weather, Space Weather Effects on Technologies, ed. P. Song, H. J. Singer, & G. L. Siscoe (Geophysical Monograph Series, Vol. 125; Washington, DC: American Geophysical Union), 11
Le Roux, J. A., Matthaeus, W. H., & Zank, G. P. 2001, GeoRL, 28, 3831
Matthaeus, W. H., Ambrosiano, J. J., & Goldstein, M. L. 1984, PhRvL, 53, 1449
Mazur, J. E., Mason, G. M., Dwyer, J. R., et al. 2000, ApJL, 532, L79
McComas, D. J., Bame, S. J., Barker, P., et al. 1998, SpSciRev, 86, 56
Melrose, D. B. 1968, Ap&SS, 2, 171
Osman, K. T., Matthaeus, W. H., Greco, A., & Servidio, S. 2011, ApJL, 727, L11
Osman, K. T., Matthaeus, W. H., Hnat, B., & Chapman, S. C. 2012a, PhRvL, 108, 261103
Osman, K. T., Matthaeus, W. H., Wan, M., & Rappazzo, A. F. 2012b, PhRvL, 108, 261102
Park, J., Moon, Y.-J., & Gopalswamy, N. 2012, JGR, 117, A08108
Reames, D. 1999, SSRv, 90, 413
Roberts, D. A., Ghosh, S., Goldstein, M. L., & Matthaeus, W. H. 1991, PhRvL, 67, 3741
Ruffolo, D., Matthaeus, W. H., & Chuychai, P. 2003, ApJL, 597, L169
Schwadron, N. A., Dayeh, M. A., Desai, M., et al. 2010, ApJ, 713, 1386
Seripienlert, A., Ruffolo, D., Matthaeus, W. H., & Chuychai, P. 2010, ApJ, 711, 980
Servidio, S., Greco, A., Matthaeus, W. H., Osman, K. T., & Dmitruk, P. 2011, JGR, 116, A09102
Smith, C. W., L'Heureux, J., Ness, N. F., et al. 1998, SpSciRev, 86, 61
Trenchi, L., Bruno, R., Telloni, D., et al. 2013, ApJ, 770, 11
Wu, P., Perri, S., Osman, K. T., et al. 2013, ApJL, 763, L30
Zimbardo, G., Pommois, P., & Veltri, P. 2004, JGR, 109, A02113
Zweibel, E. G., & Yamada, M. 2009, ARA&A, 47, 291